VIP Nanocrystal Growth

DOI: 10.1002/ange.201006412

Investigation of Indium Phosphide Nanocrystal Synthesis Using a High-Temperature and High-Pressure Continuous Flow Microreactor**

Jinyoung Baek, Peter M. Allen, Moungi G. Bawendi, and Klavs F. Jensen**

Indium phosphide (InP) nanocrystals[1] are of significant interest for use in optoelectronic devices, specifically as a replacement for CdSe nanocrystals in commercial applications. However, the current mechanistic understanding and synthetic procedures for InP nanocrystals has not yet reached the same level as for CdSe nanocrystal synthesis.[2] Using a truly continuous three-stage microfluidic reactor to precisely tune reaction conditions in the mixing, aging, and sequential growth regimes, our study described here builds on previous InP nanocrystal synthetic[3] and mechanistic work[4] to probe the significant experimental parameters involved in InP nanocrystal syntheses. We find that the growth of InP nanocrystals is dominated by the aging regime, which is consistent with a model of InP nanocrystal growth where nanocrystal growth is dominated by nonmolecular processes such as coalescence from nonmolecular InP species and interparticle ripening processes.[4] The InP growth model is in contrast to the molecular-based growth of nanocrystals as observed in CdSe and PbSe nanocrystals.[2a–f] We observe that the size of InP nanocrystals is predominantly dependent on the concentration of free fatty acid in solution and the aging temperature. Other experimental parameters such as injection temperature and particle concentration do not appear to significantly affect InP nanocrystal size or size distributions. In addition, we probe the ability to grow larger InP nanocrystals through the sequential injection of precursors in the third stage of the microfluidic reactor.

The use of high temperatures and high pressures in a continuous microfluidic system allows for a wide selection of solvents, precursors, and ligand systems, providing a vastly increased parameter space to explore synthetic conditions. The utilization of low-molecular-weight solvents at high pressures offers supercritical conditions tunable from liquid to gaslike,[5] providing high diffusion rates, improved mixing,[6] and the ability to solubilize various compounds inaccessible by solvents employed in traditional nanocrystal syntheses.[2b,c,3,7] The use of a supercritical solvent in a microfluidic reactor results in narrower residence time distributions, producing homogeneous reaction conditions ideal for nanocrystal synthesis.[8] Microfluidic systems allow precise control over reaction conditions and reproducibility[9] as a result of rigorous control of heat and mass transfer.[10] In addition, the microfluidic system can be utilized for fast screening of reaction parameters with in situ reaction monitoring.[11]

Figure 1 illustrates our truly continuous three-stage silicon-based microfluidic system consisting of mixing, aging, and sequential injection stages operating at a pressure of 65 bar,

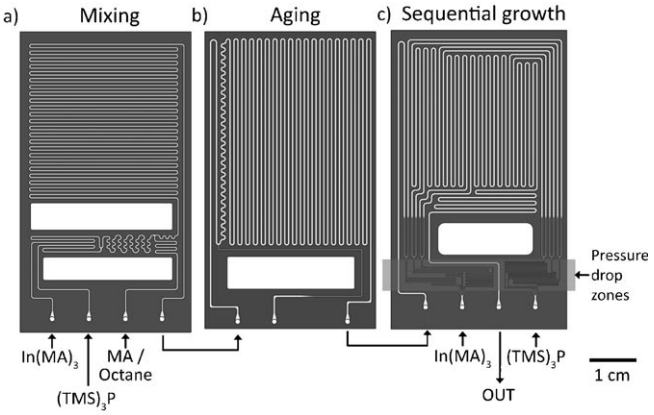

Figure 1. Three-stage high-temperature and high-pressure microfluidic system with a) a mixing stage, b) an aging stage, and c) a sequential injection microreactor with six additional injection channels. The channel widths and depths range from 80–400 μm. The sequential injection microreactor includes pressure drop zones with high flow resistance to obtain uniformly distributed injections and to prevent any backflow. TMS = trimethylsilyl.

without incorporating any manual batch manipulation between synthesis steps.[2h] We have separated each stage in order to independently probe mixing and aging processes. The first two stages of the reactor were utilized for the systematic study of InP nanocrystal formation (Figure 1 a,b). The mixing reactor was maintained at a uniform temperature to investigate the effect of different mixing temperatures. Alternatively, the first reaction stage can be heated to create a temperature gradient in order to rapidly obtain highly crystalline InP nanocrystals with relatively narrow size distributions (see Figure S1 in the Supporting Information,). The second (aging) stage of the reactor was operated at

[*] J. Baek, Prof. K. F. Jensen
Department of Chemical Engineering
Massachusetts Institute of Technology
77 Massachusetts Avenue, 66–342, MA 02139 (USA)
E-mail: kfjensen@mit.edu
Dr. P. M. Allen, Prof. M. G. Bawendi
Department of Chemistry
Massachusetts Institute of Technology
77 Massachusetts Avenue, 66–221, MA 02139 (USA)
E-mail: mgb@mit.edu

[**] The authors thank the US Army Research Office through the Institute for Soldier Nanotechnology (DAAD-19-02-0002) and the US National Science Foundation (CHE-0714189) for support. J.B. acknowledges a Samsung Scholarship from the Samsung Foundation of Culture.

Supporting information for this article is available on the WWW under http://dx.doi.org/10.1002/anie.201006412.

temperatures ranging from 200–340 °C to study the effect of aging temperature. In the third stage of the system, a sequential injection reactor (Figure 1c) was used to supply more molecular precursors for the further growth of InP nanocrystals. In the case of most InP nanocrystal syntheses, both the aging and sequential growth reactors were maintained at 320 °C to utilize supercritical octane ($T_c = 296.17$ °C and $P_c = 2.50$ MPa). Octane was selected as the solvent in order to provide excellent mixing, fast diffusivity, and sufficient density for the solubilization of all reagents.

By utilizing a two-stage microfluidic reactor (Figure 1a,b), we were able to systematically investigate the effect of different mixing and aging conditions. Notably, this separation of reaction conditions is not obtainable in a traditional benchtop set-up. Indium myristate [$In(MA)_3$] in octane was mixed with a 2:1 ratio with tris(trimethylsilyl) phosphine [$(TMS)_3P$] (see Figure S2 in the Supporting Information) at various temperatures in the first "mixing" reactor stage for 2 minutes, and subsequent aging at different reaction temperatures for 1.5 minutes in the second "aging" reactor stage. We were not able to observe a significant change in InP nanocrystal size or size distributions using a range of different mixing temperatures, with a constant aging temperature of 320 °C (Figure 2a). However, we observed an increasingly prominent first absorption feature at higher aging temperatures (Figure 2b).

The growth of InP nanocrystals appears to be largely independent of a classical "nucleation" process as the InP molecular precursors are rapidly depleted regardless of temperature.[4] These results are in stark contrast to the common models for monodisperse colloidal growth observed in CdSe nanocrystal nucleation and growth.[2f,g] In the absence of amines or other inhibiting reagents, the molecular phosphorus precursors are immediately depleted during mixing, independent of the mixing temperature. The temperature dependence of the aging process can be rationalized as the growth of InP nanocrystals being dominated by nonmolecular processes which are enhanced at higher temperatures. The nonmolecular growth of InP nanocrystals could be the cause of non-spherical InP nanocrystals, in comparison to CdSe or PbSe nanocrystals grown from molecular species. The coalescence of nonmolecular InP species may occur similarly to the recently reported coalescence growth model for gold nanoparticles.[12]

We investigated the effect of $In(MA)_3$ concentration on particle size and size distributions (Figure 2c), and found the synthesis to be largely independent of precursor or particle concentration. The independence of nanocrystal size on precursor concentration is in contrast with the behavior of II–VI CdSe nanocrystals.[8b]

Next, we sought to investigate the role of free fatty acids on particle size. As this work and previous works indicates that InP nanocrystal growth is dominated by non-molecular processes, the introduction of free fatty acids could enhance interparticle ripening processes by etching processes.[13] $In(MA)_3$ and $(TMS)_3P$ were mixed in a 2:1 ratio at 120 °C prior to the injection of excess myristic acid.

Free myristic acid was added after the depletion of molecular In and P precursors to ensure we probed the activity of carboxylic acids on interparticle ripening processes, and not promoting molecular side reactions of carboxylic acids with the molecular P precursor.[14] The aging stage was kept at a constant temperature of 320 °C, with a constant residence time of 2.7 minutes.

Figure 3a demonstrates that in the absence of free myristic acid (MA:In ratio of 3.0) the first absorption feature

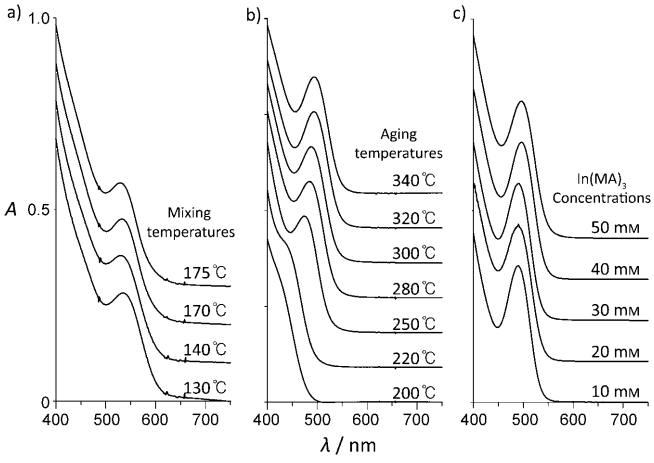

Figure 2. Absorption spectra of InP nanocrystals obtained at a variety of mixing and aging conditions. Micofluidic reactor operating with 40 mM $In(MA)_3$ and 20 mM $(TMS)_3P$ at a) different mixing temperatures followed by aging at a constant temperature of 320 °C and b) constant mixing temperature at 150 °C followed by aging at different temperatures. c) Absorption spectra with different $In(MA)_3$ concentrations using temperature gradient in the first reactor stage and a 4 min residence time with a temperature of 320 °C in the second reactor stage. Spectra are offset for clarity in (a–c); absorbances are valid for the lower spectra.

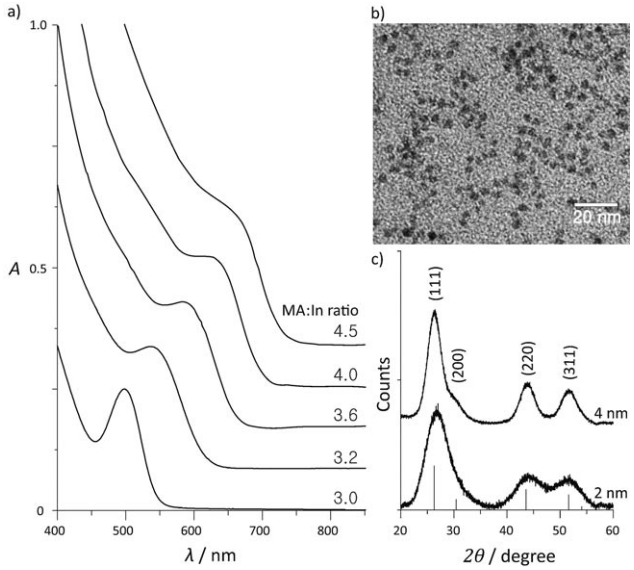

Figure 3. a) Absorption spectra of InP nanocrystals synthesized with various myristic acid to indium ratios. b) TEM image of 4 nm InP nanocrystals. c) WAXS patterns of 2 nm and 4 nm diameter InP nanocrystals. Spectra are offset for clarity in (a) and (c); absorbance/counts are valid for the lower spectra.

was located at 495 nm, corresponding to the formation of InP nanocrystals of approximately 2 nm in diameter.[15] With an increasing ratio of myristic acid to indium the first absorption feature shifted to longer wavelengths of up to 650 nm, corresponding to InP nanocrystals of 4.3 nm in diameter. The wide-angle X-ray scattering (WAXS) confirmed a zinc blende InP structure, and Scherrer analysis of the peak shapes corresponded to the appropriate InP nanocrystal crystalline coherence lengths. In addition, the InP nanocrystal size and shape was probed by transmission electron microscopy (TEM), and further corroborated our assignment of size and structure to the InP nanocrystals.

The addition of excess myristic acid was found to be the dominant experimental parameter in the control of InP nanocrystal size. The excess myristic acid may promote the dissolution of active nonmolecular InP species, such as monomers or small clusters, from the InP nanocrystal surface. The active InP species can subsequently act as a source of precursors for the growth of InP nanocrystals in a classical ripening process.[16] However, other nonmolecular processes such as the coalescence of particles may also contribute to the growth process. The drastic effect of free myristic acid on particle size is consistent with an interparticle ripening model for InP nanocrystal growth.

Another route to the synthesis of larger InP nanocrystals is the subsequent injection of additional molecular precursors. As the molecular phosphorus precursors are immediately depleted following mixing, additional injections can be a source of In or P precursors.[7] By using a method analogous to the SILAR method of overcoating nanocrystals, we alternatively supply additional monomers of $(TMS)_3P$ and $In(MA)_3$ through six injection ports. In these reaction schemes, we utilized a continuous three-stage microfluidic system which utilizes the third reactor stage for sequential injections (Figure 1c) following the mixing and aging stages. InP nanocrystals of approximately 2 nm in diameter were produced in the first two reaction stages, and then this solution was directly injected into the third sequential injection microreactor for further growth. $In(MA)_3$ and $(TMS)_3P$ were injected through six alternating subinjections. The flow resistance of each of the side injections was made to be one order higher than the resistance of the main channel by narrowing the channel widths to 80 μm and elongating the channel lengths to obtain uniformly distributed injections and to prevent any backflows. The flow resistances were calculated with a series solution of Navier–Stokes equation for rectangular channel dimensions.

Initially, InP nanocrystals were synthesized from 50 mM $In(MA)_3$ and 25 mM $(TMS)_3P$ with a 30 $\mu L\,min^{-1}$ flow rate at 320 °C aging temperature. As a result of the enhanced mixing in supercritical octane, only brief residence times were necessary between alternating injections of 80 mM of $In(MA)_3$ and 50 mM $(TMS)_3P$ (in total six injections). The amount of the additional In and P precursors that were added was controlled by tuning the injection flow rates from 5–30 $\mu L\,min^{-1}$, corresponding to a ratio of additional $(TMS)_3P$ to initial $(TMS)_3P$ ranging from 0.3–2.0. The total residence time at the sequential injection reactor varied from 1.5 minutes (for 30 $\mu L\,min^{-1}$ additional $In(MA)_3$ and $(TMS)_3P$ flows), providing a 15-second residence time per injection, and 4 minutes (for 5 $\mu L\,min^{-1}$ additional flows), providing a 40-second residence time per injection. The temperature at the additional injection points was 80 °C, and for the aging process was 320 °C. This continuous sequential injection process resulted in a growth of the first absorption peak from 495 nm to 595 nm corresponding to a size increase from 2 to 3.2 nm while maintaining a homogeneous size distribution (Figure 4). The growth of InP nanocrystals, through the method of sequential injection, allows for precise control over the growth of larger InP nanocrystals with size distributions as narrow, or narrower, than the InP nanocrystals grown by the ripening process.

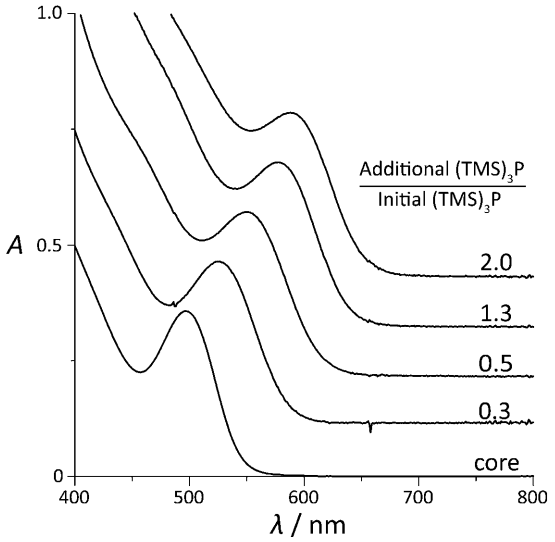

Figure 4. Absorption spectra of InP nanocrystals for various injection flow rates of $In(MA)_3$ and $(TMS)_3P$ in the sequential injection stage of the microreactor. The InP nanocrystals were synthesized using a temperature gradient in the mixing stage followed by aging at 320 °C in the aging stage. Spectra are offset for clarity; absorbance is valid for the lower spectrum.

In summary, we have developed a continuous three-stage microfluidic system that separates the mixing, aging, and subsequent injection stages of InP nanocrystal synthesis. The microfluidic system operates at high temperature and high pressure enabling the use of solvents such as octane operating in the supercritical regime for high diffusivity resulting in the production of high-quality InP nanocrystals in as little as 2 minutes. We have found that the synthesis of InP nanocrystals is largely independent of many experimental parameters that are significant in II–VI CdSe nanocrystal syntheses, such as mixing temperature and reagent concentrations. The dominant experimental parameter in the synthesis of InP nanocrystals is the concentration of free myristic acid in solution, which significantly contributes to the degree of interparticle ripening processes. We speculate InP nanocrystal growth is dominated by nonmolecular processes such as the coalescence of particles and interparticle ripening. This work will help in the design of future III–V nanocrystal syntheses, as reagents that promote interparticle ripening process may

provide a means to control the size and shape of InP nanocrystals. The further development of microfluidic systems for the synthesis of III–V nanocrystals may provide a route to synthesize III–V nanocrystals with precise control of nanocrystal size and size distributions.

Experimental Section

Microreactor fabrication: Silicon-based microreactors were prepared as previously reported.[8] Microreactors were designed from flow rate and pressure drop calculations with Matlab R2009a. Three syringe pumps (Harvard apparatus, PHD 22/2000 Hpsi, PHD Ultra Hpsi programmable, and PHD Ultra) were used for solution injections. All connections, tubes, and devices were made of type-316 stainless steel, and heating cartridges were made of multipurpose aluminium.

Preparation of precursor solutions: Octane (Sigma, anhydrous, 99%), Tri-*n*-octylphosphine (Strem, 97% min.), and all reaction solutions were dried with 4 Å molecular sieves prior to use. $(TMS)_3P$ (Strem) was used without purification. $In(MA)_3$ was prepared as previously reported.[17] The isolated $In(MA)_3$ solid was solubilized in octane solution containing 10 vol% Tri-*n*-octylphosphine.

Characterization: Absorbances were obtained by diluted InP nanocrystal solution in octane, prior to measure with Hewlett Packard 8452 diode-array spectrometer. TEM images were taken with JEOL 2010 high-resolution transmission electron microscope, and XRD data were obtained with Rigaku H3R.

Received: October 12, 2010
Published online: December 17, 2010

Keywords: indium phosphide · microfluidics · microreactors · nanocrystals · quantum dots

[1] L. Li, P. Reiss, *J. Am. Chem. Soc.* **2008**, *130*, 11588 – 11589.
[2] a) H. T. Liu, J. S. Owen, A. P. Alivisatos, *J. Am. Chem. Soc.* **2007**, *129*, 305 – 312; b) C. B. Murray, M. Nirmal, D. J. Norris, M. G. Bawendi, *Z. Phys. D* **1993**, *26*, 231 – 233; c) C. B. Murray, D. J. Norris, M. G. Bawendi, *J. Am. Chem. Soc.* **1993**, *115*, 8706 – 8715; d) N. Pradhan, D. Reifsnyder, R. G. Xie, J. Aldana, X. G. Peng, *J. Am. Chem. Soc.* **2007**, *129*, 9500 – 9509; e) L. H. Qu, X. G. Peng, *J. Am. Chem. Soc.* **2002**, *124*, 2049 – 2055; f) J. Y. Rempel, M. G. Bawendi, K. F. Jensen, *J. Am. Chem. Soc.* **2009**, *131*, 4479 – 4489; g) J. Y. Rempel, B. L. Trout, M. G. Bawendi, K. F. Jensen, *J. Phys. Chem. B* **2005**, *109*, 19320 – 19328; h) R. Kikkeri, P. Laurino, A. Odedra, P. H. Seeberger, *Angew. Chem.* **2010**, *122*, 2098 – 2101; *Angew. Chem. Int. Ed.* **2010**, *49*, 2054 – 2057; i) A. M. Nightingale, J. C. de Mello, *ChemPhysChem* **2009**, *10*, 2612 – 2614.
[3] R. Xie, D. Battaglia, X. Peng, *J. Am. Chem. Soc.* **2007**, *129*, 15432 – 15433.
[4] P. M. Allen, B. J. Walker, M. G. Bawendi, *Angew. Chem.* **2010**, *122*, 772 – 774; *Angew. Chem. Int. Ed.* **2010**, *49*, 760 – 762.
[5] C. A. Eckert, B. L. Knutson, P. G. Debenedetti, *Nature* **1996**, *383*, 313 – 318.
[6] a) A. Günther, S. A. Khan, M. Thalmann, F. Trachsel, K. F. Jensen, *Lab Chip* **2004**, *4*, 278 – 286; b) A. Günther, M. Jhunjhunwala, M. Thalmann, M. A. Schmidt, K. F. Jensen, *Langmuir* **2005**, *21*, 1547 – 1555.
[7] D. Battaglia, X. G. Peng, *Nano Lett.* **2002**, *2*, 1027 – 1030.
[8] a) S. Marre, K. F. Jensen, *Chem. Soc. Rev.* **2010**, *39*, 1183 – 1202; b) S. Marre, J. Park, J. Rempel, J. Guan, M. G. Bawendi, K. F. Jensen, *Adv. Mater.* **2008**, *20*, 4830 – 4834.
[9] H. Nakamura, Y. Yamaguchi, M. Miyazaki, H. Maeda, M. Uehara, P. Mulvaney, *Chem. Commun.* **2002**, 2844 – 2845.
[10] a) K. F. Jensen, *MRS Bull.* **2006**, *31*, 101 – 107; b) T. Gervais, K. F. Jensen, *Chem. Eng. Sci.* **2006**, *61*, 1102 – 1121.
[11] a) K. F. Jensen, *Chem. Eng. Sci.* **2001**, *56*, 293 – 303; b) K. Jähnisch, V. Hessel, H. Lowe, M. Baerns, *Angew. Chem.* **2004**, *116*, 410 – 451; *Angew. Chem. Int. Ed.* **2004**, *43*, 406 – 446.
[12] J. Polte, R. Erler, A. F. Thünemann, S. Sokolov, T. T. Ahner, K. Rademann, F. Emmerling, R. Kraehnert, *ACS Nano* **2010**, *4*, 1076 – 1082.
[13] M. Epifani, J. Arbiol, E. Pellicer, J. R. Morante, *Chem. Mater.* **2007**, *19*, 4919 – 4924.
[14] S. Xu, S. Kumar, T. Nann, *J. Am. Chem. Soc.* **2006**, *128*, 1054 – 1055.
[15] R. G. Xie, Z. Li, X. G. Peng, *J. Am. Chem. Soc.* **2009**, *131*, 15457 – 15466.
[16] C. Wagner, *Z. Elektrochem.* **1961**, *65*, 581 – 591.
[17] F. Wang, H. Yu, J. Li, Q. Hang, D. Zemlyanov, P. C. Gibbons, L. W. Wang, D. B. Janes, W. E. Buhro, *J. Am. Chem. Soc.* **2007**, *129*, 14327 – 14335.

